Effects of Accelerated Weathering Test on the Properties of Larch Wood

Liting Cheng,[a,d,*] Yajing Di,[a,d] Peng Zhao,[a,d] Jian Dai,[b,*] Zhiguo Yang,[c] and Yibin Chang [b]

To investigate the changes of larch wood properties under the influence of long-standing exposure to the environment, the QUV accelerated weathering tester (fluorescent UV and condensation testers) was used to accelerate the weathering of wood within a given preset time, and the changes were studied by analogue simulation. The wood color changed noticeably under different weathering time, and it gradually darkened from light yellow to deep reddish brown. Scanning electron microscopic (SEM) analysis revealed that as the weathering time increased, the cell wall was broken, the pits were cracked, and the tracheids were damaged. The results of the energy spectrum analysis (O/C (oxygen/carbon)) showed an increasing trend in the ratio, indicating that the wood underwent an oxidation reaction induced by light. From the values of the two testing indexes and their change patterns with weathering time, the same trend was observed, with the values of modulus of elasticity (MOE) in static bending being greater than that in dynamic bending E_d (the dynamic modulus of elasticity). However, the variability of MOE was greater than that of E_d. A comparative analysis of the two detection indicators was performed. The relationship between the proposed combined correction Ed and weathering time was: $y = 0.0000001017\ t^2 - 0.0006\ t + 9.77$.

Keywords: Accelerated weathering; Wood property; Scanning electron microscope; Nondestructive testing; Fitting

Contact information: a: The Palace Museum, Beijing 100009, China; b: Faculty of Architecture, Civil and Transportation Engineering, Beijing University of Technology, Beijing 100124, China; c: College of Petroleum Engineering, China University of Petroleum (Beijing), Beijing 102249, China; d: Key Scientific Research Base of Study and Conservation of Guanshi Architecture in Ming and Qing Dynasty, State Administration for Cultural Heritage;
** Corresponding authors: chenglting@126.com; 67393299@sina.com*

INTRODUCTION

Wood is the primary source of construction material in ancient timberwork buildings and is closely related to the character of ancient buildings. In recent years, scholars have conducted a series of studies on the changes of physical and mechanical properties of old construction wood materials and found that its properties have changed significantly due to long-term use (Huang *et al*. 2008). Due to the influence of external factors, such as biology, physics, and chemistry of the environment, ancient timberwork buildings are prone to decay and insect infestation after being used for hundreds or even thousands of years, which causes the degradation of physical and mechanical properties, and ultimately leads to the reduction of mechanical strength of ancient buildings (Xu and Qiu 2011). The study of the change of wood properties after weathering is important for the preventive conservation of wooden structures.

The aggregate structure of cellulose in wood is complex, and it easily absorbs ultraviolet (UV) light, which causes molecular chain breakage and degradation. The main functional groups of lignin, such as methoxy (-OCH_3), hydroxyl (-OH), and carbonyl (-C=O), are all light-absorbing chemical groups, which are most susceptible to UV light absorption and degradation. In addition, moisture is an important factor in accelerating the photodegradation of wood (Huang *et al*. 2013). Studies have shown that the combined effect of UV light and moisture is more conductive to the photochemical reactions within the wood than UV light alone (Altgen and Militz 2016). Wood properties are influenced by a combination of intrinsic and extrinsic factors. Recently, many studies have been conducted by domestic and foreign scholars on the weathering of wood. In terms of wood surface color change, Matsuo *et al*. (2011) studied the comparison of wood color after accelerated aging tests in historic buildings and found that the color change during natural aging is mainly a slow and mild oxidation process, and heat treatment accelerates this aging process. Thus, the color change of wood is related to the aging time. Liu *et al*. (2017) conducted aging tests on three types of wood under three sections of natural light to determine the surface color and gloss of the samples. The results showed that the wood underwent discoloration and decreased gloss after sunlight exposure, and the discoloration was more obvious. The color changes of different wood sections were different. In terms of the effect of weathering on wood properties, Lundin (2001) subjected the material to UV irradiation and found that the greatest decrease in the mechanical properties of the material occurred during the first 1000 h. The UV irradiation affected the mechanical properties of the material. Tomak *et al*. (2014) studied the changes in compressive strength, modulus of rupture, and modulus of elasticity (MOE) of four tree species during natural weathering and found that natural weathering leads to a decrease in strength properties. Gao (2016) chose Chinese fir, the most common wood for ancient buildings in Yangzhou, as the experimental material to study the change law of physical and mechanical indexes of wood during photoaging at different radiation times. It was found that the flexural MOE remained stable in the first 16 days and showed a decreasing trend after 32 days, indicating that light irradiation would change the mechanical properties of wood and there was a change law of performance indexes with time. Mohammad-Fitri *et al*. (2017) exposed glue-laminated wood to tropical climate at various times and found a decrease in density and weight, and a decrease in initial modulus of rupture. Liuyang Han *et al*. (2019) investigated the chemical and mechanical changes in the cell walls of Elm wood elements (dated from 1642 to 1681) of the ancient timberwork buildings of the Jiexiu Chenghuang Temple in Shaanxi Provincewith natural aging. After aging, the cell structure showed evident alternations, and the wood components, especially hemicellulose and lignin, were degraded, leading to deterioration of mechanical properties of aged wood compared with normal wood.

Summarizing the relevant research in recent years, it is found that the basic mechanical properties of wood, such as MOE, bending strength, and compressive strength, are affected by factors, such as environmental temperature and humidity, which eventually show changes with use time. For example, Fedyukov *et al*. (2020) have found that the physical properties (compressive strength and flexural strength) of wood structures that have been used for more than 70 years are different from those of new wood, and these changes will have an impact on the structural force performance during the whole life cycle of timber structure. Huang *et al*. (2008) took the old wood replaced during the repair of the Hall of Valor in the Imperial Palace as the test material to study the changes in the physical and mechanical properties of wood structures after more than 100 years of use and found

that their physical and mechanical properties changed due to long-term use. From the weathering mechanism of wood, there are many factors that affect wood weathering, such as light (Han *et al*. 2011), moisture (Montero *et al*. 2015), temperature, humidity (Sun *et al*. 2013), *etc*. These factors make the wood properties change greatly during the survival time. Simulating the real survival environment and studying the effects of weathering on wood properties will not only provide a reference for the formulation of building conservation and renovation plans, but also serve as a reference for the inspection, evaluation, conservation, and renovation of ancient buildings.

The purpose of this study was to evaluate the weathering properties of wood and provide a reference for the preventive protection of ancient timberwork buildings. Taking into account the principle of "minimum intervention and current protection" for ancient timberwork buildings, stress waves, and micro-drilling resistance were used. In the choice of experimental methods, nondestructive testing methods of stress wave and micro-drill resistance tester were used and compared with standard mechanical testing methods. The experimental object was the common tree species of ancient buildings - larch. The testing material was green wood, which means that it has not been used in architecture. Initially, the mechanism of wood weathering was analyzed from the perspectives of color change, scanning electron microscopy (SEM), and energy spectrum analysis of specimens. Next, the relationship between two testing indexes and weathering time of wood was analyzed from the perspectives of testing values and change trends. Finally, the comparative analysis of nondestructive and standard testing indexes was conducted, and the relationship between the dynamic modulus of elasticity (E_d) and time of larch wood was proposed to be combined and corrected.

EXPERIMENTAL

Materials

Larch wood (*Larix gmelinii*) was selected and used as the experimental material and was purchased from Eastern Royal Tombs of the Qing Dynasty Wood Factory (Tangshan City, Hebei Province, China). The diameter of the base was 50 cm, and the top was 40 cm. The height was 400 cm. The previously unused wood that was employed was approximately 300 to 400 years old. According to GB 1929 (2009), the standard for selecting specimens, each section was sawn into 2 cm × 2 cm × 36 cm specimens. The sawing method is shown in Fig. 1. According to Cheng *et al*. (2020), the selected specimens were all heartwood and had similar wood properties.

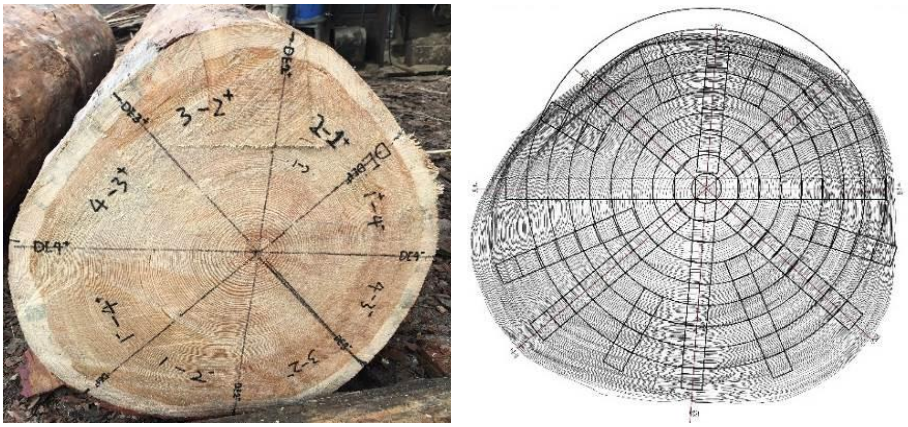

Fig. 1. Specimen sawing method

Methods

Accelerating the weathering of wood

The QUV tester QUV/spray accelerated weathering tester (Q-Lab Corporation, Cleveland, OH, USA) was used to accelerate the weathering of wood within a given preset time. The tester was divided into four boxes, labelled A, B, C, and D, with box D used as a backup. In order to reduce the error caused by the difference of moisture content (MC), the specimen was soaked to make the (MC) reach approximately 25% before the start of the test. The specimens for nondestructive test (NDT) were added to box A, and the specimens for standard test were placed into boxes B and C. The original NDT index values were measured before the accelerated weathering test and the specimens were photographed for color comparison analysis. The mass of the specimen was measured with a Lichen Technology electronic precision balance JA1003 (Shanghai Lichen Electronic Technology Co., Ltd., Shanghai, China).

The weathering conditions and time of wood treatments were set, and the weathering simulation was carried out according to the process. According to the standard ASTM G154-06 (2006), a UV lamp with a wavelength of 340 nm was selected, and the radiation intensity was set at 0.68 W/m^2, with a cycle of 12 h, in which 8 h UV irradiation at 60 (± 3) °C as blackboard temperature, 30 min water spraying, and 3.5 h condensation cycle at 60 (± 3) °C blackboard temperature. The cycle was carried out in this way.

NDT and standard testing

The testing nodes 12 h, 24 h, 36 h, 48 h, 60 h, ..., 6000 h were set, that is, the experiment was repeated 36 times. The NDT index values were measured at each testing node, using IML-RESI PD500 micro-drill resistance instrument (IML Co., Ltd., Wiesloch, Germany) and FAKOPP microsecond timber (FAKOPP Enterprise Bt., Ágfalva, Hungary). Additionally, the specimens were photographed after each test.

The time of standard test indexes was set according to the NDT data, the testing nodes 336 h, 504 h, 720 h, 1080 h, 1332 h, 1572 h, 1716 h, 1950 h, 2204 h, 2424 h, 2600 h, 2960 h, 3368 h, 3752 h, 4328 h, and 5528 h were set. The following testing methods, GB/T 1935 (2009), GB/T 1936.2 (2009), and GB/T 1936.1 (2009), were carried out using a universal testing machine (Jinan Ruima Machinery Equipment Co., Ltd., Jinan, China).

According to Eq.1, the moisture content was calculated,

$$MC=\frac{(M-M')}{M'}\times 100\% \quad (1)$$

where MC is the moisture content (%), M is the mass after weathering (g), and M' is the mass before weathering (g).

According to Eq.2, the density values was calculated,

$$\rho=\frac{M}{V} \quad (2)$$

where ρ is the density (g/cm^3), M is the mass(g), and V is the volume(cm^3).

SEM and energy spectrum analysis testing

Specimens were removed at various time points after artificial accelerated weathering. The following procedure of analysis occurred, such as slicing, pasting, evacuating, gold spraying, and scanning electron microscope (SEM)-energy spectrum analysis. To ensure the consistency, the samples were taken from the central part of the weathering specimens.

In the slicing procedure, a small knife was used to cut a section of the specimen facing the UV surface, the size of the section should not exceed 5 mm × 5 mm × 3 mm, and the surface should be flat and smooth.

In the pasting procedure, the samples were glued to the experimental table, leaving a gap between the samples for easy differentiation.

In the evacuating and gold-spraying procedure, a Leica EM SCD500 (Leica Microsystems, Wetzlar, Germany) was used to spray metal coating on the surface of SEM samples, which is convenient for electron microscope observation.

In the scanning procedure, the SEM was used to analyze the surface microstructure of wood before and after UV accelerated weathering, using a FEI QUNGTA 200 scanning electron microscope (FEI Company, Hillsboro, OR, USA). It was also equipped with EDAX Genesis 2000 X-ray spectrometer (EDS), which can analyze the composition of the specimen.

RESULTS AND DISCUSSION

Appearance of Color and SEM Analysis

Color appearance

To ensure consistency in color comparison, the same exposed surface was used for color comparison of appearance under various weathering times, as shown in Fig. 4. The color was light yellow before weathering, slightly darkened at 492 h, and noticeably darkened at 1008 h. The color deepened gradually from 1008 h to 2960 h, showing a deepened reddish-brown state, slightly darkened at 3368 h, and further darkened to a deep reddish-brown color from 3368 h to 5528 h.

During weathering, the samples were exposed to UV irradiation, water spraying, and condensation, and the changes of light, moisture, and temperature also occurred. The MC increased from 30% to 50%. The color changes that occur in wood may be related to photochromism, chemical discoloration, or their interaction. It has been shown that the main factor causing photochromism in wood is UV light (Budakci 2006). When irradiated by UV light, the covalent bonds of polymeric compounds in wood break, which in turn generates various free radicals that quickly combine and react with oxygen, and then go

through a radical intermediate called hydroperoxide, which in turn generates photosensitive radicals that cause discoloration of wood (Muasher and Sain 2006). Heitner (1993) studied the photodegradation of lignin and found that lignin after photodegradation generates water-soluble products that eventually produce chromogenic functional groups, which lead to yellowing and discoloration of wood. Kallakas *et al*. (2015) studied the effect of UV radiation on the mechanical and physical properties of wood-plastic composites (WPCs) and found that the color of WPCs became lighter after UV radiation treatment. Kropat *et al*. (2020) summarized relevant studies on wood color changes under natural weathering; the relevant research content and research results were summarized and explained in detail. It was pointed out that the wood's initial color will be influenced by drying conditions, thermal treatments, and periods of storage.

As a result of the color change after UV irradiation, water spraying, and the interaction of both can cause a change in the color of the material. As the weathering time increases, the wood undergoes degradation after the alternating effects of light, water spray, and high temperatures.

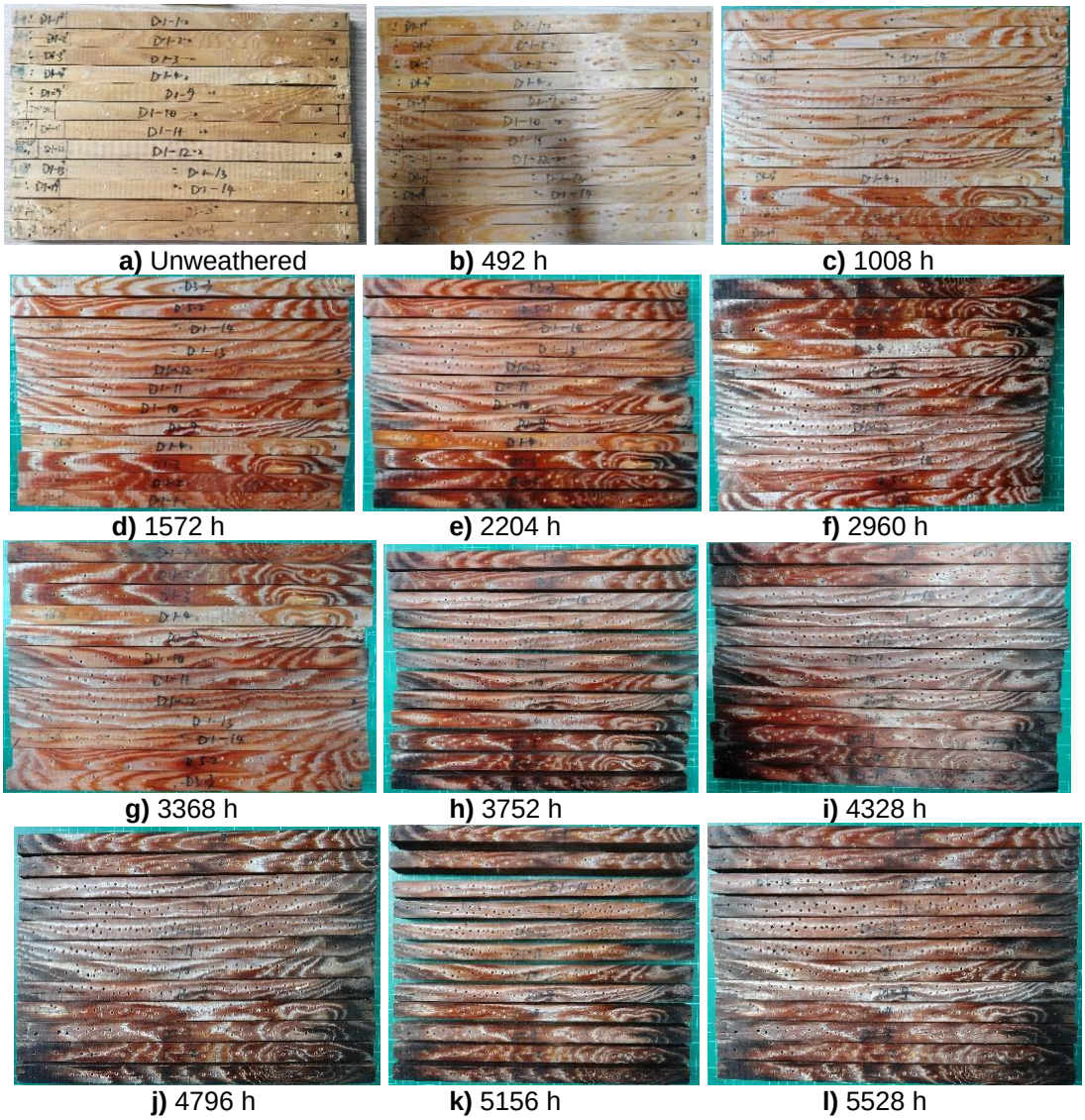

Fig. 2. Change of color with weathering time

SEM and Energy Spectrum Analysis

The results of the SEM analysis of the specimens with increasing weathering time are shown in Fig. 3.

The SEM micrographs of larch indicated that the cell walls were intact and free of debris in cross-sections of wood that had not been subjected to accelerated weathering. Figure 3a shows a clear and complete outline of the cell walls. The rimmed pores can be clearly seen in the radial section of the cell, and the pores are clear and clean. The part similar to the crassula is clearly visible at the upper and lower edges of the striae, and the cell walls of the tubular cells are intact and free of vestiges. With increasing weathering time in the radial section, the initially intact tubular cells were gradually broken. In the transverse section, the cell wall has been broken. The scanned images show that the surface of the wood had degraded to a certain extent after weathering. Damage to the cell walls, and abrasion or breakage of the grain pores, such as fissures and thickened threads, can be seen in the duct walls.

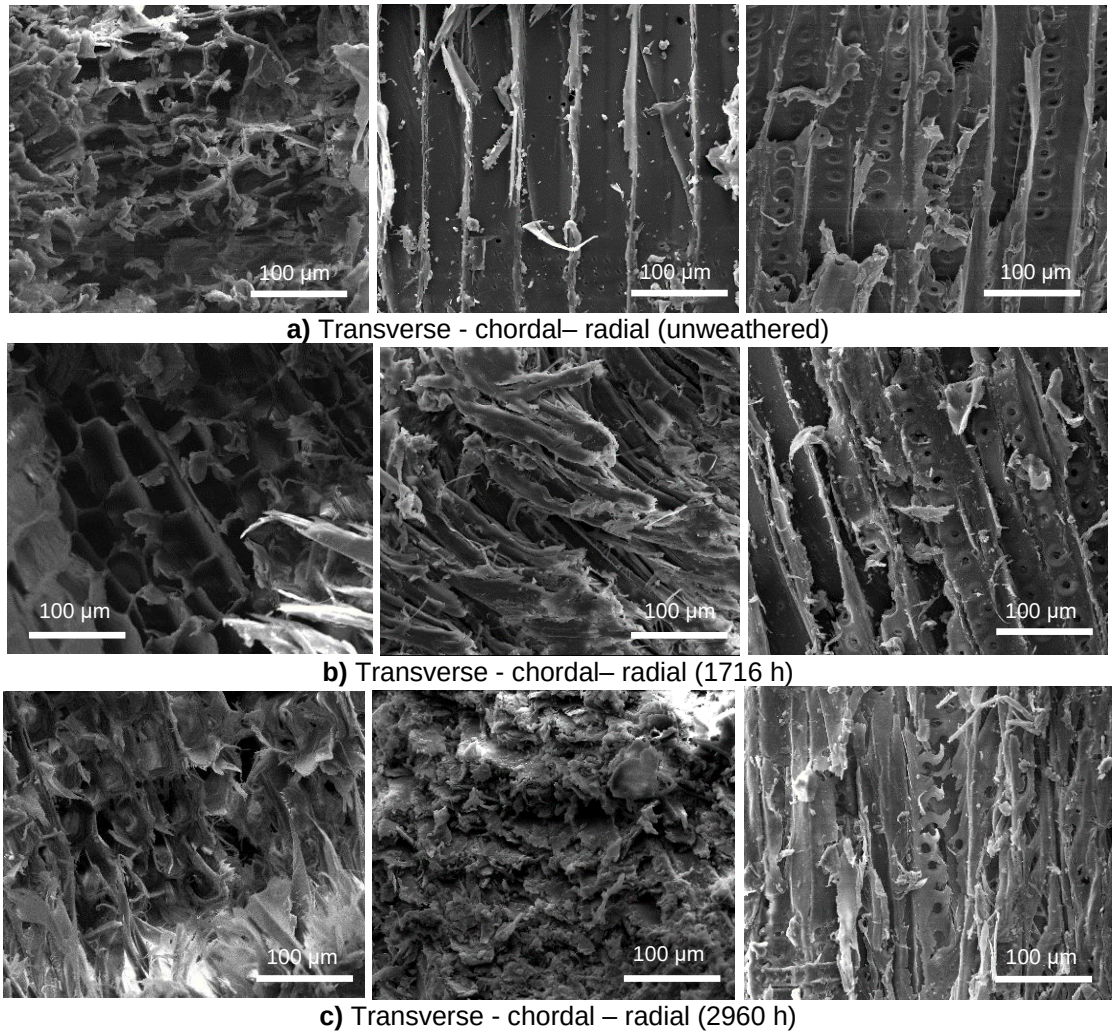

a) Transverse - chordal– radial (unweathered)

b) Transverse - chordal– radial (1716 h)

c) Transverse - chordal – radial (2960 h)

Fig. 3. SEM images for different artificial weathering times

The surface composition of the specimen material changes after a certain time of weathering treatment, and the EDS test allows the comparison of the changes in the type and content of elements on the surface of the material before and after weathering (Yu 2015). High resolution XPS scans were performed on the specimens before weathering, and the scans showed that the main elements on the surface before weathering were C, O, and H. The mass and the percentages of O/C content on the surface before and after weathering of the specimens are shown in Fig. 4.

The trend of O/C with weathering time reveals that the mass and the quantity percentages underwent a gradual increase, with values ranging from 0.9 to 1.19 for the mass percentage, and from 0.73 to 0.9 for the quantity percentage. The increase of O/C may be related to the degradation of lignin in the wood during UV irradiation. Hon *et al*. (1986 and 1982) thought that the lignin undergoes an oxidation reaction induced by light. After oxidation more oxygen content appears on the surface of the wood. At the same time, during the degradation of wood cellulose, unstable carbon radicals were generated, which were dehydrogenated in the presence of oxygen, and thus formed peroxide radicals, which then underwent a series of chain reactions to generate peroxides. Reinprecht *et al*. (2018) found that lignin was susceptible to breakdown when irradiated by UV light.

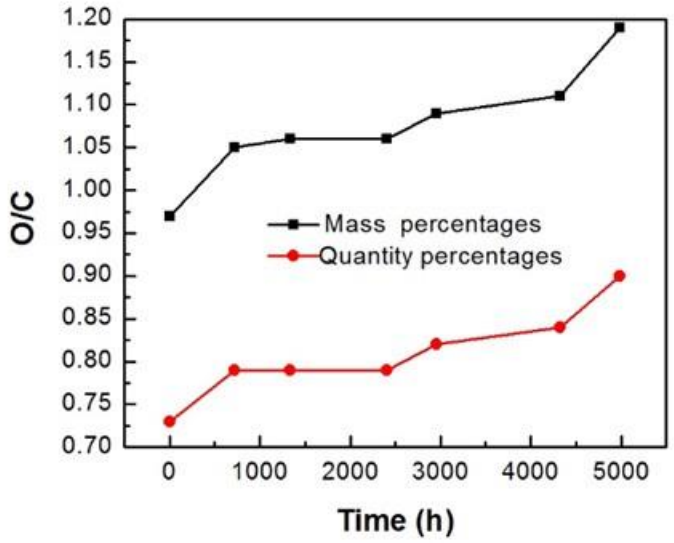

Fig. 4. Energy spectrum analysis of O/C content with weathering time

Figure 5 shows the schematic diagram of the energy spectrum analysis for unweathered and 4328 h artificially weathered specimens.

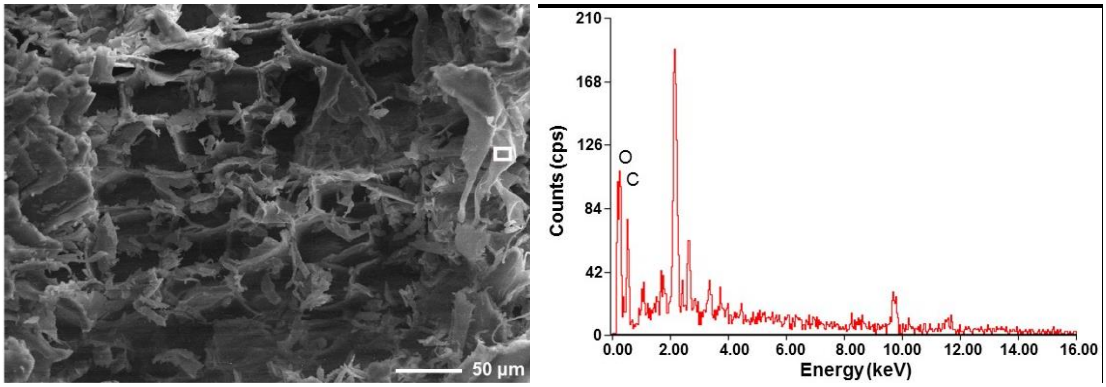

a) Unweathered

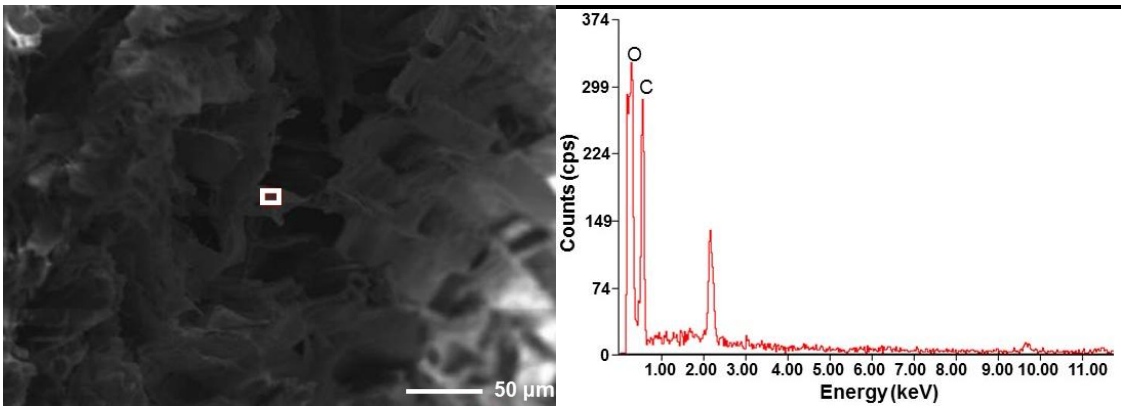

b) 4328 h

Fig. 5. Results of energy spectrum analysis at different weathering time

Changes of Testing Indexes under Nondestructive Testing Method

The relationship between NDT indexes (the indexes obtained by NDT technology) and weathering time is shown in Fig. 6. It can be seen from the figure that with the increase of weathering time, MC and density showed gradual increasing trends, and the stress wave propagation velocity, the modulus of stress-resistograph of the drilling needle (the product of the square of the stress wave propagation velocity and the rotational resistance value of the drilling needle, F_{drill}), and the modulus of stress-resistograph of the feeding needle (the product of the square of the stress wave propagation velocity, and the resistance value of the feeding needle, F_{feed}) showed decreasing trends. The E_d showed fluctuation.

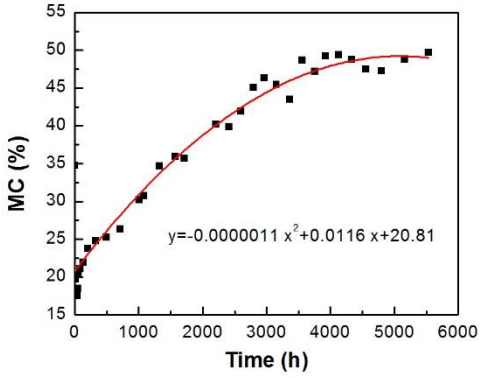

a) MC

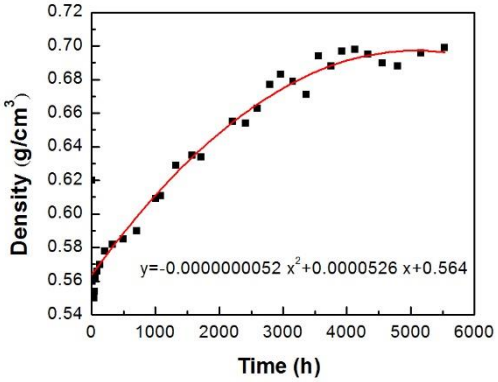

b) Density

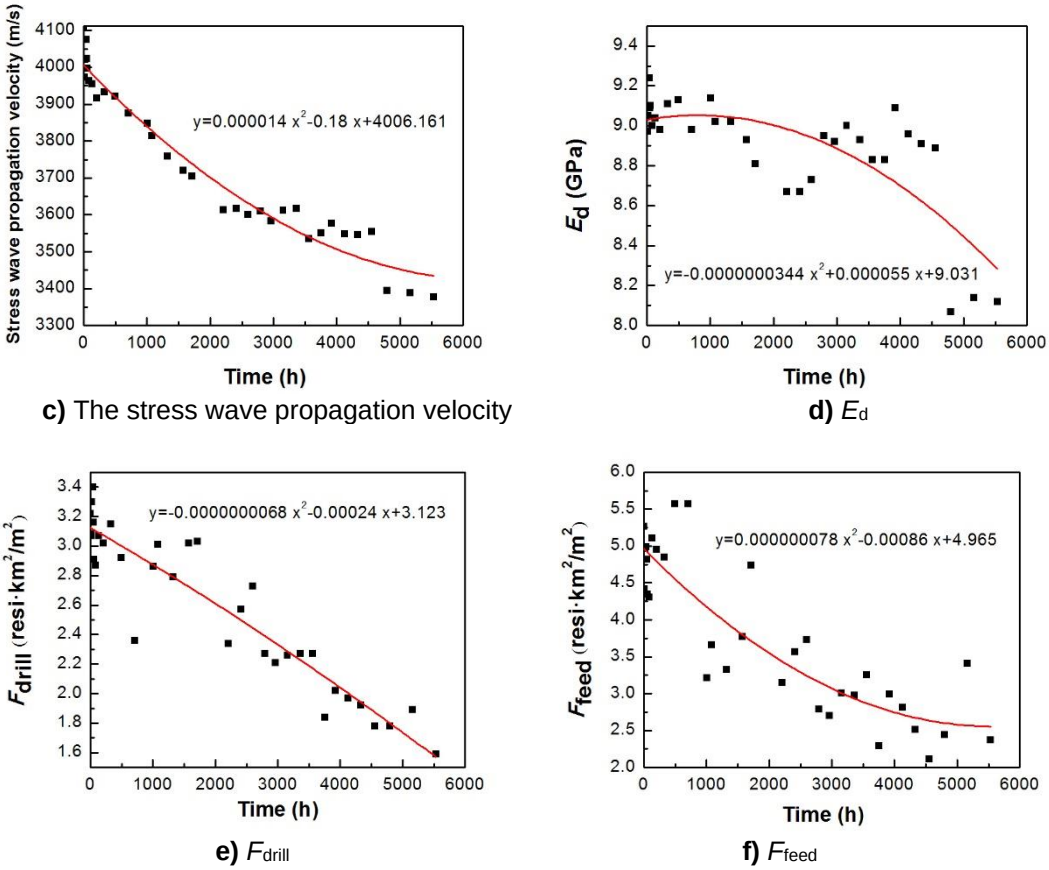

Fig. 6. The relationship between nondestructive testing indexes and weathering time

The growth rates of MC and F_{drill} increased continuously before 4000 h, and fluctuated after 4000 h. The growth rates of density and F_{feed} showed a continuous increase. During the weathering time, various material property indicators displayed some complicated fluctuations, which may be due to the oxidation and degradation of cellulose, hemicellulose, lignin, and the migration of extracts. This led to fluctuations in material properties.

The above changes in the NDT indexes may be the result of changes in the microstructure of the wood. The cell wall of wood is the substantial bearing structure of wood, where cellulose microfibrils are the reinforcing phase, whereas lignin and hemicellulose form the matrix laminate structure. The distribution of cellulose, hemicellulose, and lignin in the cell wall, the way they are bound, and the properties of the components themselves noticeably influence the cell wall and the macroscopic mechanical properties of the wood (Zhang 2011). When wood is subjected to the cyclic effects of UV radiation, water spray, and high temperatures, the cell wall structure, distribution, and binding patterns of wood are damaged, and degradation of cellulose, hemicellulose, and lignin occurs, resulting in changes in the wood testing indexes. Scholars have done some relevant studies. For example, Han (2012) thought the swelling effect of water increases the space for material reaction in wood, thus increasing the possibility of photochemical reaction. Altgen *et al*. (2016) thought that under the combined action of moisture and ultraviolet light, the photochemical reaction in wood is easier.

The SEM results are shown in Fig. 7. In Fig. 7(a), the striae are clearly visible and the cell wall is intact without breakage, while in Fig. 7(b), the striae are visible but are cracked or even broken and the cell wall has a broken structure. Figure 7(a) shows the wood when it is not artificially weathered, and Fig. 7(b) is artificially weathered for 3000 h. The wood shown in Fig. 7(a) had a MC of approximately 18%, a density of approximately 0.5 g/cm^3, a stress wave propagation velocity of approximately 4000 m/s, an E_d of approximately 9.8 GPa, an F_{drill} of approximately 3.3 resi·km^2/m^2, and an F_{feed} of about 4.97 resi·km^2/m^2. The wood shown in Fig. 7(b) had a MC of about 45%, a density of about 0.68 g/cm^3, a stress wave propagation velocity of about 3500 m/s, an E_d of about 8.8 GPa, an F_{drill} of about 2 resi·km^2/m^2, and an F_{feed} of about 3 resi·km^2/m^2. From the comparison of the two sets of data, the variability of the values of the individual properties is remarkable. It may be related to the degradation of cellulose, hemicellulose, and lignin at 3000 h in the wood. With weathering time, the degradation of lignin and hemicellulose in the wood cell wall occurs, which makes the interaction forces between the main components of the cell wall gradually weaken (Sumiya *et al*. 1967). This to some extent causes damage to the integrity of the cell wall. In the cell wall, hemicellulose forms an interfacial polymer, which is an interfacial coupling agent between cellulose and lignin and plays an important linking role, considerably affecting the elastic modulus of the cell wall. The mechanical properties of wood are highly correlated to the cell wall structure. The hardness of the cell wall changes with the changes of the main chemical components of the cell wall, which gradually decreases with the degradation of lignin and hemicellulose, and the degradation of these chemical components makes the cell wall less resistant to permanent deformation, thus showing that changes in the microstructure of wood have a noticeable effect on wood properties. Guo *et al*. (2019) pointed out that cellulose, hemicellulose, and lignin, which are chemical components of the wood cell wall, are important factors affecting wood strength, such as wood hardness, elastic modulus, and strength. Fei (2014) thought that the hardness of the cell wall decreased with the decrease of lignin and hemicellulose.

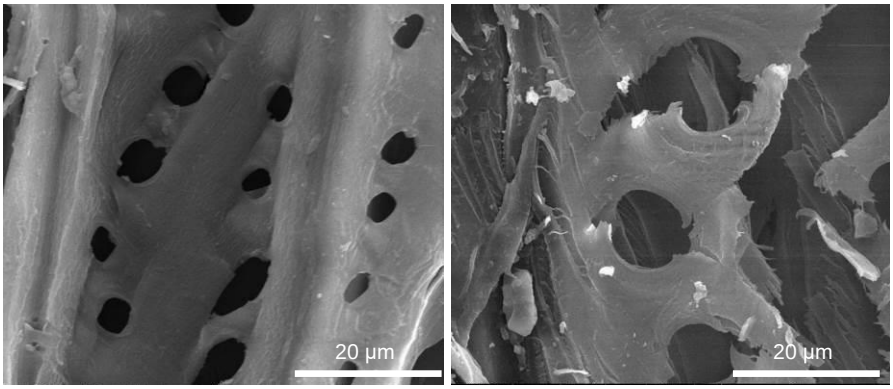

a) Unweathered **b)** 3000 h

Fig. 7. Comparison of SEM at different weathering times

Changes of Testing Indexes Under Standard Testing Method

The standard testing indexes (the indexes measured by the standard mechanical test method) at various weathering times were measured. The trends and relationship with weathering time are shown in Fig. 8. The figure shows a general downward trend. There were occasional fluctuations during the period.

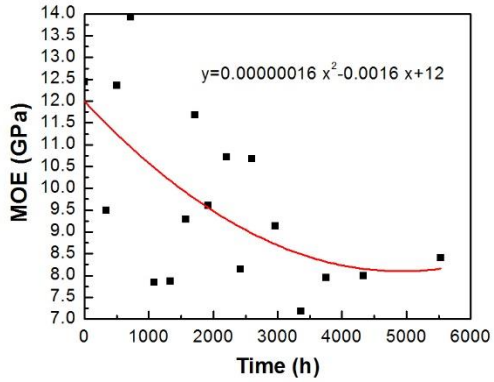

a) MOE in static bending

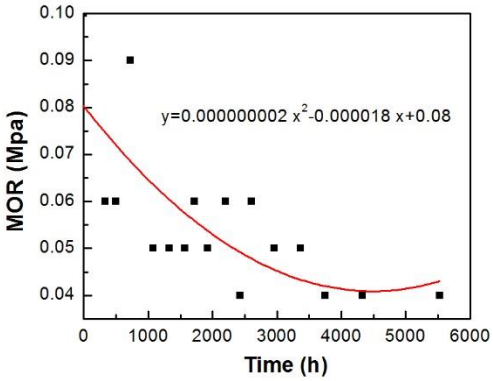

b) Bending strength (MOR)

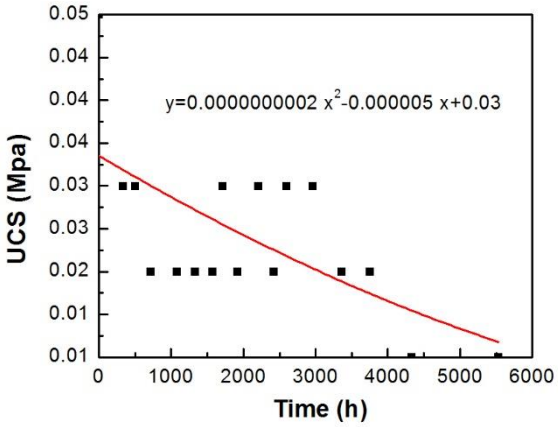

c) Compressive strength parallel to the grain (UCS)

Fig. 8. Trends and relationships of standard testing indexes with time

Comparison of E_d and MOE

From the trend of change, the test results for both E_d and MOE showed a gradual decrease in elastic modulus with weathering time. As shown in Fig. 9, the values of MOE were greater than E_d, and the maximum difference was about 5.0 GPa. In terms of fluctuation range, MOE was greater than E_d, and the maximum fluctuation of the NDT results was 1.0 GPa, while the maximum fluctuation value measured by the standard testing method was about 6 GPa. In comparison with MOE, the trend of change presented by E_d is not obvious.

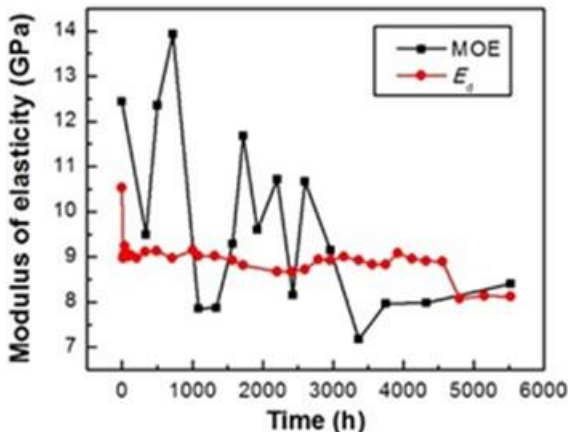

Fig. 9. The comparison of the results of the two testing methods

The difference between MOE and E_d was fitted to obtain a curve, which is shown in Fig. 10. The MOE was used to correct the E_d versus time, and the relationship between the proposed combined correction E_d and weathering time was: $y = 0.0000001017t^2 - 0.0006t + 9.77$.

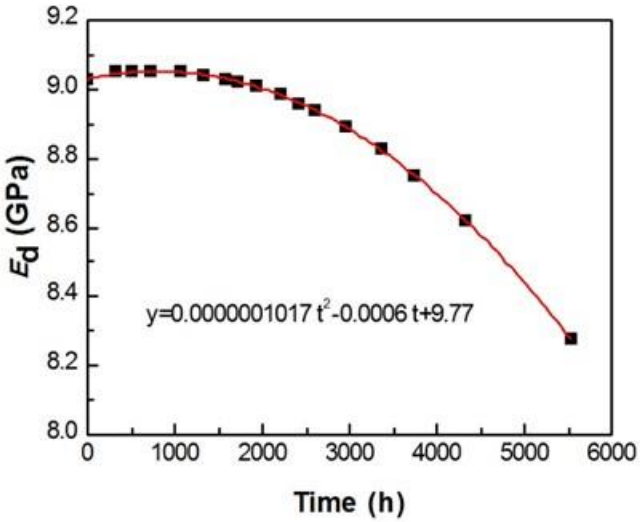

Fig. 10. The modified relationship between E_d and weathering time

CONCLUSIONS

1. The color appearance of the larch wood changed noticeably at various artificial weathering times. It gradually deepened from light yellow to dark reddish brown.
2. The scanning electron microscopy (SEM) results at different weathering time showed that, with increasing weathering time, the cell walls had broken down in the transverse section and the grain pores appeared to be fractured. In the radial section, there was breakage of the tubular cells.

3. In terms of the trend of change, the two testing results showed the same trend. Numerically, modulus of elasticity (MOE) was greater than the dynamic modulus of elasticity (E_d), but the volatility of MOE was greater than E_d. The relationship between the proposed combined correction E_d and weathering time was: $y = 0.0000001017t^2 - 0.0006t + 9.77$.

ACKNOWLEDGMENTS

The authors are grateful for the support of the National Key R&D Program (2019YFC1520902 and 2020YFC1522402).

REFERENCES CITED

Altgen, M., and Militz, H. (2016). "Photodegradation of thermally-modified Scots pine and Norway spruce investigated on thin micro-veneers," *European Journal of Wood and Wood Products* 74(2), 185-190. DOI: 10.1007/s00107-015-0980-3

ASTM G154-06 (2006). "Standard practice for operating fluorescent light apparatus for UV exposure of nonmetallic materials," ASTM International, West Conshohocken, PA, USA.

Budakci, M. (2006). "Effect of outdoor exposure and bleaching on surface color and chemical structure of Scots pine," *Progress in Organic Coatings* 56(1), 46-52. DOI: 10.1016/j.porgcoat.2006.01.018

Cheng, L., Dai, J., Yang, Z., Qian, W., Wang, W., Wang, Z., and Gao, Z. (2020). "Variation of larch wood property indexes based on nondestructive testing data," *BioResources* 15(2), 2906-2923. DOI: 10.15376/biores.15.2.2906-2923

Fedyukov, V., Chernov, V., and Chernova, M. (2020). "Strength of aged wood in old constructions," *Journal of Applied Engineering Science* 18(1), 114-119. DOI: 10.5937/jaes18-23002

Fei, B. (2014). *Characterization Technology and Application of Wood Cell Wall Mechanical Properties*, Science Press, Beijing, China.

Gao, Y. (2016). *The Degeneration on Mechanical Properties of Aged Wood and Corresponding Damage Constitutive Model*, M. S. Thesis, Yangzhou University, Yangzhou, China.

GB/T 1929 (2009). "Method of sample logs sawing and test specimens selection for physical and mechanical tests of wood," Standardization Administration of China, Beijing, China.

GB/T 1935 (2009). "Method of testing in compressive strength parallel to grain of wood," Standardization Administration of China, Beijing, China.

GB/T 1936.1 (2009). "Method of testing in bending strength of wood," Standardization Administration of China, Beijing, China.

GB/T 1936.2 (2009). "Method for determination of the modulus of elasticity in static bending of wood," Standardization Administration of China, Beijing, China.

Guo, Y., Li, C., Li, Y., Wang, Z., and Yao, L. (2019). "Research progress on the relationship between wood cell wall and wood mechanical properties and moisture

properties," *China forest products industry* 46(8), 14-18. DOI:10.19531/j.issn 1001-5299.201908004

Han, Y., Li, Y., and Zhou, Y. (2011). "Wood photodegradation mechanism and its research advances," *World Forestry Research* 24(4), 35-39. DOI: 10.13348/j.cnki.sjlyyj.2011.04.002

Han, Y. (2012). *Study on Colorfastness to Light of Wood and Modified Wood*, M.S. Thesis, Chinese Academy of Forestry, Beijing, China.

Han, L., Wang, K., Wang, W., Guo, J., and Zhu, H. (2019). "Nanomechanical and topochemical changes in Elm wood from ancient timber constructions in relation to natural aging," *Materials* 12(5), article no. 786. DOI: 10.3390/ma12050786

Heitner, C. (1993). "Light-induced yellowing of wood-containing papers," in: *Photochemistry of Lignocellulostic Materials*, Volume 531, American Chemical Society, Washington D.C., USA, pp. 3-25. DOI: 10.1021/bk-1992-0531.ch001

Hon, D. N. S., and Feist, W. C. (1986). "Weathering characteristics of hardwood surfaces," *Wood Science and Technology* 20(2), 169-183. DOI: 10.1007/BF00351028

Hon, D. N. S., and Feist, W.C. (1982). "Participation of singlet oxygen in the photodegradation of wood surfaces," *Wood Science and Technology* 16(3), 193-201. DOI:10.1007/BF00353868

Huang, R., Jin, H., Shi, Z., Xia, R., Li, H., and Liu, X. (2008). "Study on physico-mechanical properties of ancient architecture of the Palace Museum," in: *The 1st National Biomass Materials Science and Technology Symposium*, Beijing, China, pp. 502-507.

Huang, X., Kocaefe, D., Kocaefe, Y., Boluk, Y., and Krause, C. (2013). "Structural analysis of heat-treated birch (*Betula papyrifera*) surface during artificial weathering," *Applied Surface Science* 264, 117-127. DOI: 10.1016/j.apsusc.2012.09.137

Kallakas, H., Poltimäe, T., Süld, T. M., Kers, J., and Krumme, A. (2015). "The influence of accelerated weathering on the mechanical and physical properties of wood-plastic composites," *Proceedings of the Estonian Academy of Sciences* 64(1S), 94-104. DOI: 10.3176/proc.2015.1S.05

Liu, R., Pang, X., and Yang, Z. (2017). "Measurement of three wood materials against weathering during long natural sunlight exposure," *Measurement* 102, 179-185. DOI: 10.1016/j.measurement.2017.01.034

Lundin, T. (2001). *Effect of Accelerated Weathering on the Physical and Mechanical Properties of Natural-fiber*, M. S. Thesis, University of Wisconsin, Madison, WI, USA.

Kropat, M., Hubbe, M. A., and Laleicke, F. (2020). "Natural, accelerated, and simulated weathering of wood: a review," *BioResources* 15(4), 9998-10062.

Matsuo, M., Yokoyama, M., Umemura, K., Sugiyama, J., Kawai, S., Gril, J., Kubodera, S., Mitsutani, T., Ozaki, H., and Sakamoto, M. (2011). "Aging of wood: Analysis of color changing during natural aging and heat treatment," *Holzforschung* 65(3), 361-368. DOI: 10.1515/hf.2011.040

Mohammad-Fitri, K., Zaidon, A., Lee, S. H., Nabil-Fikri, L., and Edi-Suhaimi, B. (2017). "Effects of accelerated and outdoor ageing on leachability and properties of compreg-laminated sesenduk wood," *Journal of Tropical Forest Science* 29(2), 198-207.

Montero, M. J., De la Mata, J., Esteban, M., and Hermoso, E. (2015). "Influence of moisture content on the wave velocity to estimate the mechanical properties of large

cross-section pieces for structural use of Scots pine from Spain," *Maderas. Ciencia y Tecnología* 17(2), 407-420. DOI: 10.4067/S0718-221X2015005000038

Muasher, M., and Sain, M. (2006). "The efficacy of photostabilizers on the color change of wood filled plastic composites," *Polymer Degradation and Stability* 91(5), 1156-1165. DOI: 10.1016/j.polymdegradstab.2005.06.024

Reinprecht, L., Nosal', E., Panek, M., and Kacik, F. (2018). "The impact of natural and artificial weathering on the visual, colour and structural changes of seven tropical woods," *European Journal of Wood and Wood Products* 76(1), 175-190. DOI:10.1007/s00107-017-1228-1

Sumiya, K., Nomura, T., and Yamada, T. (1967). "Creep and infrared spectra of chemically treated Hinoki wood," *Materials* 16(169), 830-833. DOI: 10.2472/jsms.16.830

Sun, Y., Yang, L., and Que, Z. (2013). "Influence of temperature on the properties of wood," *Anhui Agricultural Science Bulletin* 19(16), 109-111. DOI: 10.16377/j.cnki.issn 1007-7731.2013.16.005

Tomak, E., Ustaomer, D., Yildiz, S., and Pesman, E. (2014). "Changes in surface and mechanical properties of heat-treated wood during natural weathering," *Measurement* 53, 30-39. DOI: 10.1016/j.measurement.2014.03.018

Xu, M., and Qiu, H. (2011). "Experimental study on properties of aged wood of ancient architecture," *Earthquake Resistant Engineering and Retrofitting* 33(4), 53-55. DOI: 10.3969/j.issn.1002-8412.2011.04.009

Yu, H. (2015). *Analysis on Mechanism of Bamboo UV Photo Aging*, Ph.D. Dissertation, Chinese Academy of Forestry, Beijing, China.

Zhang, S. (2011). *Chemical Components Effect on Mechanical Properties of Wood Cell Wall*, Ph.D. Dissertation, Chinese Academy of Forestry, Beijing, China.

Article submitted: July 6, 2021; Peer review completed: September 5, 2021; Revised version received and accepted: September 7, 2021; Published: September 17, 2021.
DOI: 10.15376/biores.16.4.7400-7415